Nonlinear dynamic fractional sliding mode control to the motor of mining locomotive

ZHANG Hai-ming[1], MIAO Zhong-cui[2], ZHANG Xin[2]

(1. *School of Automation and Electrical Engineering, Lanzhou Jiaotong University, Lanzhou 730070, China*;
2. *School of Mechanical and Electrical Engineering, Lanzhou Jiaotong University, Lanzhou 730070, China*)

Abstract: The harsh operating environment and complex operating conditions of the mine electric locomotive affect the control performance of the locomotive traction motor. In order to improve the speed control performance of electric locomotive traction motors, a dynamic fractional-order sliding mode control(DFOSMC) algorithm considering uncertain factors was proposed. A load torque sliding mode observer was designed for the complex load disturbance of the traction motor, and its observations were integrated into the DFOSMC controller to overcome the influence of load disturbance. Finally, the stability of the designed controller was proved by Lyapunov's theorem. Besides, the control performance of DFOSMC controller was compared with integer-order sliding mode controller and fractional-order sliding mode controller through simulation experiments. Compared with integer-order sliding mode and fractional-order sliding mode controllers, the dynamic and static performance of the DFOSMC controller with load observation is better, and it has stronger anti-interference ability. The DFOSMC controller effectively improves the control performance of the traction motor of the mining locomotive.

Key words: mine electric locomotive; fractional-order sliding mode; load observer; dynamic fractional-order sliding mode control (DFOSMC)

CLD number: TP273; TD64 **doi**: 10.3969/j.issn.1674-8042.2020.04.009

0 Introduction

With the rapid development of national railways, highways and other infrastructure construction, the application and demand of mining electric vehicles for production and construction are increasing. However, mining locomotives have low technical content, high failure rate and high energy consumption. Therefore, it is urgent to improve the traction control performance of mining locomotives.

The mining locomotive is a narrow-gauge electric locomotive, and its traction control and power parts are on the traction locomotive. The overall structure and track of the traction locomotive is simple, and it is often in the state of frequent starting, braking and acceleration and deceleration. The locomotive must adapt to the complex road conditions such as uphill and downhill operations, bumps caused by uneven tracks and so on. This increases the difficulty of locomotive traction control and raises higher control requirements.

Traction control of mining locomotives has mainly gone through three stages: DC series excitation series resistance, DC series excitation chopping and AC frequency conversion speed regulation[1]. Due to its own structural advantages and high-performance variable frequency speed control, AC motors gradually replace DC traction motors and are widely used in mining locomotive traction[2-4]. The traction characteristics of mining locomotives should include large starting torque, strong overload and anti-jamming capability. Therefore, higher requirements are placed on the control of traction motors.

Vector control is a high-performance AC frequency conversion speed control method. Its speed controller generally adopts PI strategy. But PID is a linear control method, and its robustness is poor. It can only meet the requirements within a certain range, and it is difficult to meet the requirements of high performance control [5]. In recent years, fuzzy controller[6], neural network controller [7], sliding mode controller (SMC) [8] and other advanced control methods have been applied to the field of AC motor control. In contrast, SMC has the characteristics of

Received date: 2020-10-14

Foundation items: National Natural Science Foundation of China (No. 51867012)

Corresponding author: MIAO Zhong-cui (1109326877@qq.com)

strong robustness, insensitivity to system parameters and external disturbances, fast response and simple algorithm. It is particularly suitable for application in the field of motor control. However, the disadvantage of sliding mode control is chattering during sliding mode motion. Chattering would damage the operating components, reduce the operating life of the system, and increase the extra energy consumption of the system. Therefore, in order to reduce chattering, Chern et al introduced the integral term in the sliding mode surface, which not only effectively weakened chattering, but also reduced the steady-state error[9]. However, due to large initial error or actuator saturation, the integral saturation effect of the integer order integral sliding surface would lead to large overshoot and long regulation time, which leads to the deterioration of the dynamic performance [10].

Fractional calculus is applied to the field of control, which expands the description ability of integer order calculus. In recent years, along with the study of the fractional calculus theory, fractional integral increases the degree of freedom of integral calculation. Not only fractional integral has memory characteristics, but also its memory characteristics decay with time. Combining fractional integration with sliding mode control can effectively reduce conventional sliding mode chattering and improve the dynamic performance of sliding mode control and other qualities[11]. In Refs. [11-13], better control performance has been achieved by combining fractional order integral and sliding mode control.

Based on the above analysis, considering the severe working environment of the mining traction motor and serious load disturbance, the fractional-order integral sliding mode control algorithm is applied to the speed controller of the vector control system of the mining traction motor. Furthermore, for the uncertain factors such as parameter changes in the vector control system of mining traction motors, a dynamic fractional-order integral sliding mode control (DFOSMC) algorithm considering uncertain nonlinearities is proposed. In order to improve the robustness of the traction control system against load disturbances, a traction motor load torque observer is designed, and the observed value is fed back to the DFOSMC controller in real time. Finally, the operating conditions of the mining electric locomotive is simulated to verify the calculated control system.

1 Fractional order theory

As we know, ${}_aD_t^\alpha$ is the basic operator of fractional calculus, which is defined as

$$ {}_aD_t^\alpha = \begin{cases} \mathrm{d}^\alpha/\mathrm{d}t^\alpha, & \mathrm{Re}(\alpha) > 0 \\ 1, & \mathrm{Re}(\alpha) = 0 \\ \int_a^t (\mathrm{d}\tau)^{-\alpha}, & \mathrm{Re}(\alpha) < 0, \end{cases} \tag{1} $$

where α is the order; $\mathrm{Re}(\alpha)$ is the real part; a and t are the upper and lower bounds of the operator, respectively.

In the development of fractional calculus theory, there are many definitions of fractional calculus, and its rationality and scientific definition have been verified in practice. At present, there are two kinds of definitions that are most commonly used[14].

Definition 1: (type GL) Grunwald-Letnikov fractional calculus definition is expressed as

$$ {}_aD_t^\alpha f(t) = \lim_{h\to 0} h^{-\alpha} \sum_{j=0}^{(t-\alpha)/h} (-1)^j \binom{\alpha}{j} f(t-jh), \tag{2} $$

where $(t-\alpha)/h$ represents rounding operation; h is the step size; $\binom{a}{j}$ is a binomial coefficient, and it can be expressed as

$$ \binom{a}{j} = \frac{\alpha(\alpha-1)(\alpha-1)\cdots(\alpha-j+1)}{j!} = \frac{\alpha!}{j!(\alpha-j)!}. \tag{3} $$

Definition 2: (type RL) Riemann-Liouville fractional calculus definition is expressed as

$$ {}_aD_t^\alpha f(t) = \frac{1}{\Gamma(m-\alpha)} \left(\frac{\mathrm{d}}{\mathrm{d}t}\right)^m \int_\alpha^t \frac{f(\tau)}{(t-\tau)^{1-(m-\alpha)}} \mathrm{d}\tau, \tag{4} $$

where m is an integer, $m-1<\alpha<m$, $m\in N$.

If the initial value of the function $\varepsilon>0$ and its derivatives is 0, the Laplace transform defined by RL is transformed into

$$ L\{{}_aD_t^\alpha f(t)\} = s^\alpha F(s). \tag{5} $$

2 Mathematical model of asynchronous motor

The following assumption is made when establishing the mathematical model of asynchronous motor: The magnetic potential of the motor is sinusoidal along the circumference of the air gap; Ignoring the saturation of magnetic circuit; the self-inductance and mutual inductance of each winding are

constant, ignoring the influence of iron loss[15].

According to the assumptions, the mathematical model of asynchronous traction motor is established in the synchronously rotating m-t orthogonal coordinate system.

The voltage vector equation is expressed as

$$\begin{cases} u_s = R_s i_s + \dfrac{\mathrm{d}}{\mathrm{d}t}\psi_s + \mathrm{j}\omega_1 \psi_s, \\ 0 = R_r i_r + \dfrac{\mathrm{d}}{\mathrm{d}t}\psi_r + \mathrm{j}(\omega_1 - \omega)\psi_r, \end{cases} \tag{6}$$

where u_s is stator voltage vector; i_s and i_r are stator and rotor current vectors, respectively; ψ_s and ψ_r are stator and rotor flux vectors, respectively; R_s and R_r are stator and rotor resistance values, respectively; ω_1 is synchronous speed of motor, and ω is motor rotor speed.

According to the rotor flux oriented m-t rotating coordinate system, to ensure that the m-axis and rotor flux vector coincide, then

$$\begin{cases} \psi_{rm} = \psi_r, \\ \psi_{rt} = 0, \\ \dfrac{\mathrm{d}\psi_{rt}}{\mathrm{d}t} = 0. \end{cases} \tag{7}$$

The dynamic equation of electromagnetic torque under the constraint of magnetic field is

$$T_e = n_p \frac{L_m}{L_r} i_{st} \psi_r. \tag{8}$$

3 Design of DFOSMC controller

The traction motor motion equation is expressed as

$$T_e - T_L = \frac{J}{n_p}\frac{\mathrm{d}\omega_r}{\mathrm{d}t}, \tag{9}$$

where T_L is the load torque, J is the moment of inertia of the motor (including the motor and the load).

Considering the robustness of the control system to uncertain factors such as parameter changes and various disturbances, the speed controller is designed as an integral sliding mode control type. Considering the influence of uncertain factors in the control system, the equation of motion is expressed as which

$$\dot{\omega}_r = (b + \Delta b)T_e - (b + \Delta b)T_L, \tag{10}$$

where $b = \dfrac{n_p}{J}$, and Δb is the impact of system uncertainties.

The speed error of the system can be defined as

$$x(t) = \omega_r^* - \omega_r, \tag{11}$$

where ω_r^* is the given speed value. Then the state equation of the motor can be obtained as

$$\dot{x}(t) = -\dot{\omega} = -(b + \Delta b)T_e + (b + \Delta b)T_L = -bT_e + bT_L + \eta, \tag{12}$$

where η is the influence of uncertainties such as system internal parameter changes and external disturbances.

According to Eq. (12), DFOSMC speed controller can be designed, and the steps are as follows.

1) Design of sliding surface for DFOSMC.

2) Design of control rate.

The dynamic sliding surface ensures system control performance. And the control rate is to ensure that the system state quickly reaches the sliding mode surface, that is, the system achieves better control performance by overcoming the influence of various uncertain factors.

3.1 Design of DFOSMC sliding surface

The integral sliding mode surface can improve the accuracy and robustness of the controller[16], and it is expressed as

$$s = x(t) + c\int x(t)\mathrm{d}t, \tag{13}$$

where c is a constant, $c>0$. The greater the c value, the faster the speed response.

The sliding surface defined by Eq. (13) is the integral order integral sliding surface. The integral of the speed error is global integral. When the initial error is relatively large, the effect of the integral will affect the speed performance of the traction motor. In order to solve this problem, a fractional order sliding surface is presented as

$$s = x(t) + cD_t^{-\alpha}x(\tau), \tag{14}$$

where α is the fractional order, $0<\alpha<1$.

According to the definition of fractional order calculus RL type

$${}_0D_t^{-\alpha}x(t) = \frac{1}{\Gamma(m-\alpha)}\int_0^t (t-\tau)^{(m-\alpha)-1}x(\tau)\mathrm{d}\tau = \frac{1}{\Gamma(m-\alpha)}\int_0^t \Phi(t-\tau)x(\tau)\mathrm{d}\tau, \tag{15}$$

where $\Phi(t-\tau) = (t-\tau)^{(m-\alpha)-1}$ is the weight function of the error integral, the weight function has the properties as[10]

$$\lim_{t\to 0^+}\Phi(t) = +\infty, \quad \lim_{t\to+\infty}\Phi(t) = 0^+. \tag{16}$$

Fractional integration is the accumulation of

deviations after acting on weight functions. According to Eq. (16), it can be seen that the weight of the fractional order integral is the initial error that cumulatively decreases with time.

To further suppress the sliding mode chattering, combining fractional integral and dynamic sliding mode, the sliding mode surface is designed as

$$\begin{cases}\delta = \dot{s} + \lambda s, \\ s = x(t) + cD_t^{-\alpha}x(\tau), \end{cases} \tag{17}$$

where λ is a strictly normal number, which is related to the rapidity of the system state approaching the sliding mode surface.

The initial state is $x(0)=0$ and $\delta(0)=0$. That is, $\dot{s}+\lambda s=0$ is a progressively stable first-order dynamic system. It can be seen that the initial state of the control system is on the sliding mode surface, and there is no approach process for the sliding mode control law. Therefore, the control system is globally robust.

3.2 Design of control law

In order to ensure the stability of the control system, the control law of DFOSMC consists of two parts and is expressed as

$$\hat{T}_e = T_{eq} + \Delta T_e, \tag{18}$$

where T_{eq} is the equivalent control law, which keeps the system state on the sliding mode surface under the action of equivalent control law and makes the system fast and stable; ΔT_e is the switch control, which is defined as

$$\Delta T_e = \eta \mathrm{sgn}(\delta) + \varepsilon\delta, \tag{19}$$

where η is the switching gain, which means that the rate of arrival of the switching surface; $\varepsilon>0$ is an exponential term, driving the state to reach the switching surface.

After derivation of Eq. (17), substituting Eq. (12) into it, we can get

$$\dot{\delta} = -b\hat{T}_e + \lambda\dot{x}(t) + cD_t^{2-\alpha}x(\tau) + c\lambda D_t^{1-\alpha}x(\tau) + b\hat{T}_L + \dot{\eta}. \tag{20}$$

Then the control law is obtained as

$$\hat{T}_e = \frac{\lambda}{b}\dot{x}(t) + \frac{c}{b}D_t^{2-\alpha}x(\tau) + \frac{c\lambda}{b}D_t^{1-\alpha}x(\tau) + \hat{T}_L - \varepsilon\mathrm{sgn}(\delta) - \zeta\delta. \tag{21}$$

3.3 Stability proof and analysis

To prove the stability of DFOSMC, reasonable assumptions are made as follows.

Hypothesis 1: Uncertainty is bounded, and there is a bounded function $B_n(x)$, which can be expressed as

$$|\eta| \leqslant B_n(x), \ \forall x \in \mathbf{R}^n. \tag{22}$$

Hypothesis 2: The derivative of the uncertainty factor is bounded, and it can be expressed as

$$|\dot{\eta}| \leqslant \bar{B}_n(x), \ \forall x \in \mathbf{R}^n. \tag{23}$$

Hypothesis 3: There is a positive real number ε that satisfies $\varepsilon > \bar{B}_n$.

In order to prove the stability of the designed controller, the Lyapunov function needs to be defined as

$$V = \frac{1}{2}\delta^2. \tag{24}$$

From Eqs. (20) and (21), we can easily get the following expression as

$$\dot{\delta} = -b\hat{T}_e + \lambda\dot{x}(t) + cD_t^{2-\alpha}x(\tau) + c\lambda D_t^{1-\alpha}x(\tau) + \dot{\eta} = \dot{\eta} - \varepsilon\mathrm{sgn}(\delta) - \zeta\delta. \tag{25}$$

When $\zeta>0$, according to hypothesis 1 to 3, the derivative of V is given as

$$\dot{V} = \delta\dot{\delta} = \delta(\dot{\eta} - \varepsilon\mathrm{sgn}(\delta) - \zeta\delta) = \delta\dot{\eta} - \varepsilon|\delta| - \zeta\delta^2 < \delta\dot{\eta} - \varepsilon|\delta| < \delta\dot{\eta} - \bar{B}_n|\delta| < 0. \tag{26}$$

That is, the stability of the DFOSMC controller can be guaranteed.

4 Design of load observer

4.1 Design of load observer

In view of the complexity of the load disturbance of the locomotive traction motor, a sliding mode observer is proposed to observe the load disturbance signal in real time. The observed value is integrated into the DFOSMC controller to suppress load disturbance.

The rate of change of T_L can be ignored during the control period, namely $\dot{T}_L=0$. According to Eq. (7), the equation of state can be obtained as

$$\begin{cases}\dot{\omega}_r = bT_e - bT_L, \\ \dot{T}_L = 0. \end{cases} \tag{27}$$

To observe the load torque T_L of the traction motor, the sliding mode observer is designed as

$$\begin{cases}\dot{\hat{\omega}}_r = bT_e - b\hat{T}_L + U, \\ \dot{\hat{T}}_L = gU, \end{cases} \tag{28}$$

where $\hat{\omega}_r$ is the observed value of speed; $\hat{T}_L$ is the observed value of load torque; g is the gain of

feedback; $U=k_1\mathrm{sgn}(\hat{\omega}-\omega)$ and k_1 is the gain of sliding mode.

Subtracting Eqs. (27) from (28), the sliding mode observation error can be obtained as

$$\begin{cases}\dot{e}_1=-ke_2+U,\\ \dot{e}_2=gU,\end{cases}\tag{29}$$

where $e_1=\hat{\omega}-\omega$ is the speed observation error, $e_2=\hat{T}_\mathrm{L}-T_\mathrm{L}$ is the load torque observation error, and the sliding mode switching surface is define as

$$s=e_1.\tag{30}$$

4.2 Stability analysis

In order to prove the stability of the load observer, the Lyapunov function is defined as

$$V(s)=\frac{1}{2}s^2.\tag{31}$$

1) Because of $s=e_1$, we can get

$$\dot{s}=\dot{\hat{\omega}}-\dot{\omega}=kT_\mathrm{e}-k\hat{T}_\mathrm{L}+U-kT_\mathrm{e}+kT_\mathrm{L}=-ke_2+k_1\mathrm{sgn}e_1.\tag{32}$$

When $s\dot{s}<0$ satisfies the sliding mode accessibility condition, the derivative of V is given as

$$\dot{V}=s\dot{s}=e_1(-ke_2+k_1\mathrm{sgn}e_1)\leqslant 0.\tag{33}$$

After simplification, the value range of k_1 should meet $k_1\leqslant -k|e_2|$.

2) When $s=\dot{s}=0$, speed observation error satisfies $e_1=\dot{e}_1=0$. From Eq. (29), it can be obtained as

$$\begin{cases}U=ke_2,\\ \dot{e}_2=gU,\end{cases}\tag{34}$$

which is also expressed as

$$\dot{e}_2-gke_2=0.\tag{35}$$

According to the stability theory, the condition that the system can be stabilized is $-gk>0$. Due to $k=\frac{n_\mathrm{p}}{J}>0$, $g<0$ can be determined. It can be seen from Eq. (35) that the load torque observation error e_2 approaches zero in an exponential function, and the approach rate is determined by g.

In summary, when $k_1\leqslant -k|e_2|$ and $g<0$, $\dot{V}\leqslant 0$. That is, the designed load observer is stable and it can accurately observe the load torque.

5 Simulation experiment

In order to verify the effectiveness of the designed controller, a simulation model of the traction motor vector control system was built according to Fig. 1.

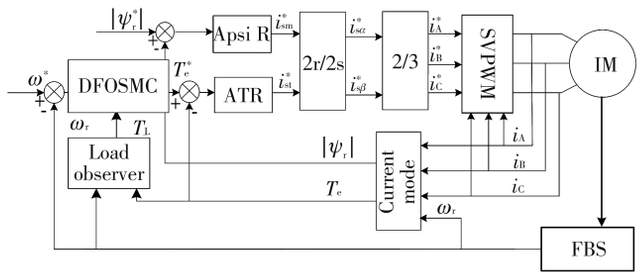

Fig. 1 Vector control block diagram of mining asynchronous traction motor

In order to verify the performance of the DFOSMC, the DFOSMC, fractional integral sliding mode (FOSMC) and integer integral sliding mode (SMC) were simulated and compared. Table 1 presents the related parameters of the motor.

Table 1 Traction motor parameters

Parameter	Value	Unit	Description
V	380	V	Rated voltage
f	50	Hz	Frequency
n	1 400	r/min	Rated speed
R_s	1.850	Ω	Stator resistance
R_r	2.658	Ω	Rotor resistance
L_m	0.283 8	H	Mutual inductance
L_s	0.294 0	H	Stator self-inductance
L_r	0.289 8	H	Rotor self-inductance
P	2		Number of poles
J	0.142 5	kg·m^2	Motor Inertia

In the simulation, ATR and ApsiR are PI controllers. The corresponding parameters are $K_\mathrm{pATR}=3.5$, $K_\mathrm{iATR}=1.2$, $K_\mathrm{pApsiR}=300$ and $K_\mathrm{iApsiR}=100$, respectively. The relevant parameters used in the simulation are shown in Table 2.

Table 2 Related parameters

Parameter	Value	Description
k	−400	Load observer sliding mode gain
g	−20	Load observer feedback gain
λ	80	Constant in DFOSMC
c	100	Constant in DFOSMC
α	0.3	Order of fractional integration
ζ	0.015	DFOSMC switching gain
ε	0.8	DFOSMC approaching constant

5.1 Simulation experiment of load torque observer

Firstly, the load torque observation performance of the traction motor was tested, and the observation value was integrated into DFOSMC, as shown in Fig. 2. Then a load of 10 N·m was suddenly added at 0.45 s, and disappeared at 0.60 s. It can be seen that the observer can quickly and accurately observe and follow the change of the actual load and then

become stabilized.

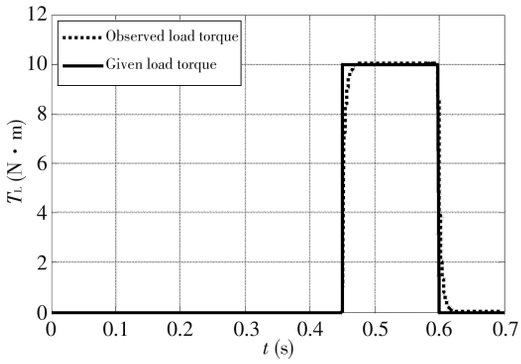

Fig. 2 Observed response curve of sudden increase load

After validating the rationality and accuracy of the sliding mode observer, load torque observations can be incorporated into the DFOSMC speed controller.

5.2 Step by step accelerated operation

In actual operation, the speed control of the electric locomotive is generally multi-gear control. When starting, the gear control handle is pushed from the position "0" to "1", and the locomotive is slowly started. After all vehicles are started, the control handle is evenly pushed to positions 2, 3, etc., and the locomotive accelerates evenly to a given speed. When simulating acceleration step by step, different speeds were given according to different times. The results for the DFOSMC, FOSMC and SMC are illustrated in Fig. 3.

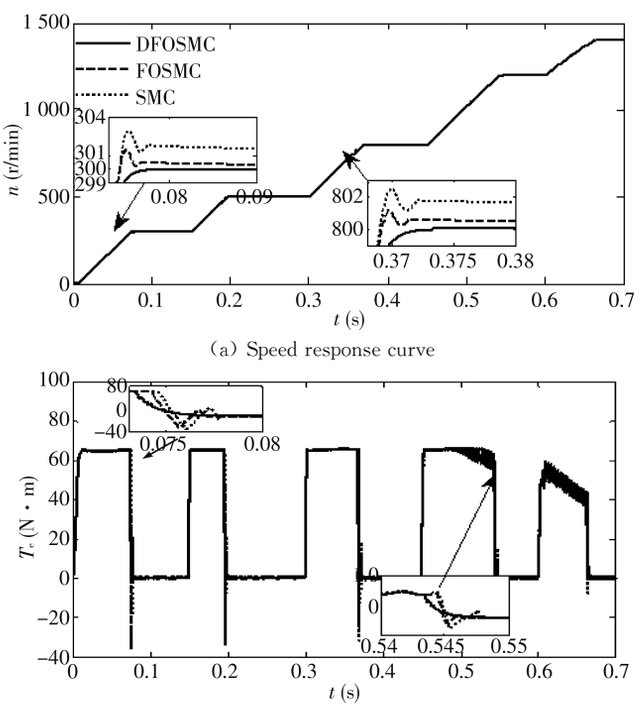

(a) Speed response curve

(b) Torque response curve

Fig. 3 Speed/torque response curves of speed increased step by step

Among the three speed controllers, the speeds of FOSMC and SMC controllers have overshoot. In comparison, the steady-state error of SMC is the largest, and there is torque ripple when reaching a given speed. The rotation speed of DFOSMC is the smoothest and eliminated the torque ripple.

5.3 Start without load and sudden increase or decrease of load

In the simulation, the sudden increase and decrease of load were used to simulate the road bumps and sudden changes in basic resistance during operation of the electric locomotive. As shown in Fig. 4, t = 0 s—0.34 s is the starting process of the motor. At t = 0.34 s, the locomotive reaches the rated speed and starts to run at a constant speed. When t = 0.45 s, a sudden load of 10 N · m is applied. After the speed is reduced, it quickly rises to near the rated speed. Compared with the three controllers in Fig. 4, DFOSMC has the fastest speed response, without overshoot and the smallest steady error when the traction motor reaches given speed.

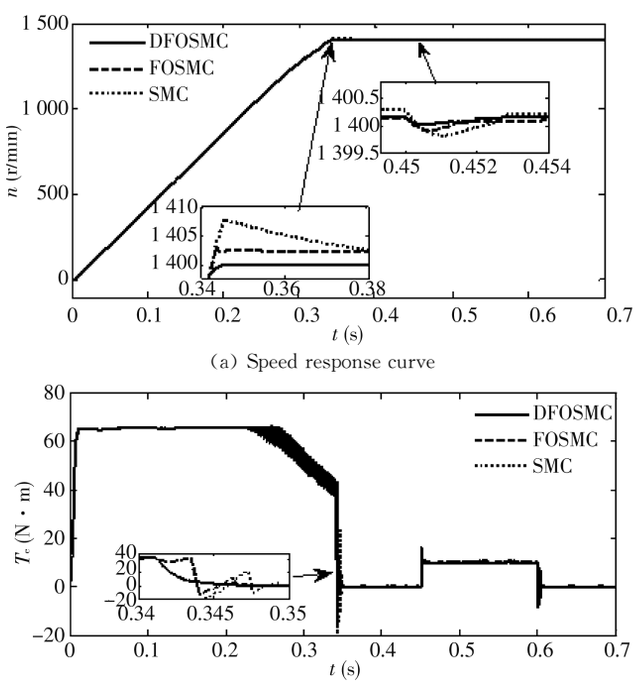

(a) Speed response curve

(b) Torque response curve

Fig. 4 Speed/torque response curves when load suddenly increases or decreases

When the load is suddenly added in 0.45 s, the speed of DFOSMC is basically unchanged, while the dynamic drop value of FOSMC and SMC control speed is larger and the recovery time is longer. From the electromagnetic torque waveform, the electromagnetic torque response curve of DFOSMC is smoother without pulsation around 0.34 s. Thus,

the speed of DFOSMC is the most stable and has the strongest resistance to load interference.

5.4 Run at low speed and full load

In the simulation, the traction motor was started with a rated load of 20 N·m, the given speed was 500 r/min, and a sudden load of 10 N·m was added at 0.45 s, which was to simulate the additional load caused by mechanical collision and road bumps when the electric locomotive runs stably. Fig. 5 shows the speed and electromagnetic torque response curves of the three controllers. Comparing the three controllers, when DFOSMC reaches given speed, there is no overshoot, and it can quickly stabilize, and the electromagnetic torque quickly reduces to the rated load torque without overshoot. When the load is suddenly added at 0.45 s, the speed of DFOSMC reduces quickly, but it returns to the original speed quickly. While the recovery time of FOSMC and SMC is longer. The simulation results show that the traction motor based on DFOSMC control is more stable at low speed and full load, the electromagnetic torque response is faster, the speed is smoother without overshoot, and the anti-interference performance is stronger.

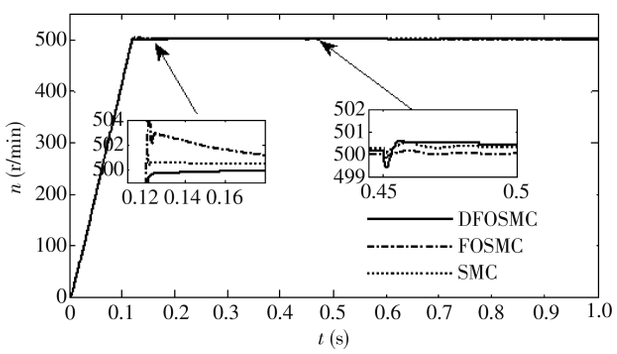

(a) Speed response curve

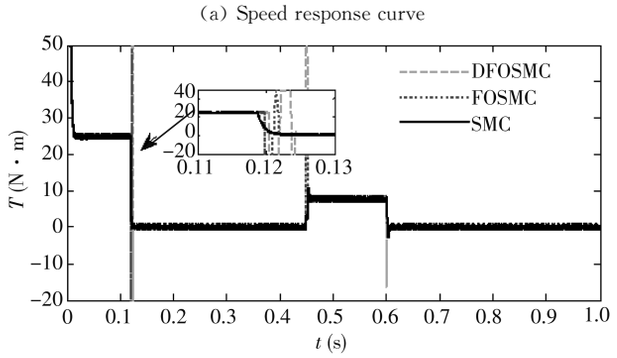

(b) Torque response curve

Fig. 5 Speed/torque response curves of low speed rated load operation

5.5 Full load and climbing

Due to the complicated terrain of the electric locomotive, the running track generally has a ramp, and the electric locomotive may run on a slope. Sometimes the electric locomotive may stay on the slope. Fig. 6 shows the response curves of speed and torque when simulating the low-speed full-load climbing of the mine electric locomotive. If the traction motor starts with 2.5 times the rated load (including rated load and additional resistance load), at this time, since the traction motor cannot overcome the load torque, the cooperation of the mechanical brake device is required, otherwise it will reverse. In the simulation, the mechanical braking action was simulated in the interval of $t=0$ s—0.20 s to keep the locomotive speed at 0 r/min. After the torque overcame the load torque, the mechanical brake device was released, and the electric locomotive started to climb.

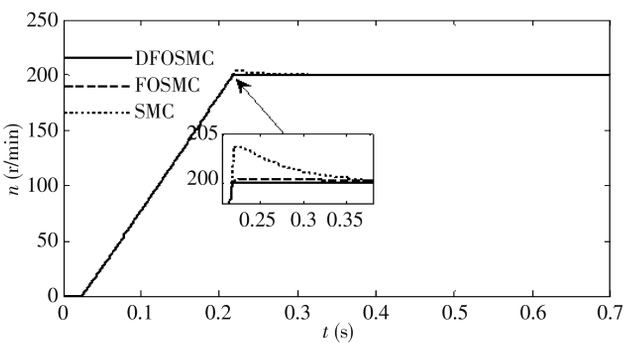

(a) Speed response curve

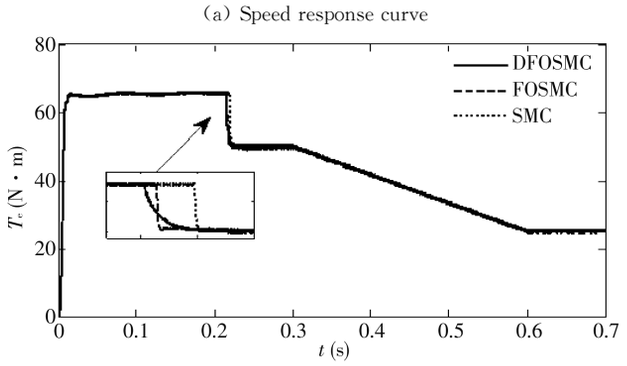

(b) Torque response curve

Fig. 6 Speed/torque response curves of low speed rated load climbing operating

As shown in Fig. 6, the electromagnetic torque overcomes the load torque at 0.20 s, and the motor starts to increase at a constant torque. When the speed reaches a given speed of 200 r/min, the electromagnetic torque rapidly decreases to the load torque, and the electric locomotive starts to run at a constant speed on the ramp. The tractor reaches the top of the ramp at 0.31 s, and the loaded vehicles arrives in turn. As the full loaded vehicles reach the top of the ramp in sequence, the additional resistance load of the locomotive gradually decreases. At 0.6 s,

the last loading vehicle runs to the top of the ramp, and the climbing operation of electric vehicle ends and then runs at a constant speed. The traction motor reaches the given speed at 0.22 s. Comparing FOSMC with SMC, it can be seen that the speed of DFOSMC has no overshoot and the smallest steady error, the electromagnetic torque response is the fastest and stabilizes quickly. And the traction motor remains smoothly when the load changes. It is verified that the DFOSMC control has a fast response speed and good stability.

6 Conclusion

In view of the harsh working environment of the mine electric locomotive and the complexity of load interference, in our work, the following improvements have been made for the speed controller of the traction motor of the mining locomotive, and the feasibility and effectiveness of the proposed method are verified by simulation experiments.

1) The DFOSMC speed controller is proposed. The dynamic fractional integral sliding mode surface greatly weakens the sliding mode chattering and accelerates the arrival time. By comparing FOSMC with SMC, the response speed of the system is improved, and the chattering and overshoot of the system are significantly reduced.

2) A load torque sliding mode observer is designed, and the observation of load torque is integrated into the DFOSMC controller, which improves the system's anti-load interference ability.

3) Simulating the different running conditions of mining locomotives, the designed DFOSMC is compared with FOSMC and SMC, respectively. Simulation experiments show that the DFOSMC controller proposed has the fastest response speed, no overshoot characteristics, and the steady error was significantly reduced. By comparing FOSMC with FOSMC, the DFOSMC speed controller with load observer effectively improves the control performance of the mining locomotive traction motor.

References

[1] Zong J, Ruan Y, Xu L B. Simulation of mine traction electrical locomotive control system. Motor and Control Applications, 2013, 40(8): 14-18.

[2] Yang G, Geng H, Wang H G. A Torque control strategy of induction motors taking efficiency of dynamic state into account. Journal of Electrotechnical Society, 2005, 20(7): 93-99.

[3] Feng G, Qi W, Zhang B, et al. Analysis and comparison of three-phase variable frequency PMSM with single-phase induction motor in house hold appliances. In: Proceedings of 2011 International Conference on Electrical Machines and Systems. Beijing: IEEE Press, 2011: 1-5.

[4] Li Z K, Ruan Y, Zong J, et al. Design of variable frequency speed regulation control system for dc stringing electric mine locomotive. Motor and Control Applications, 2011, 38(5): 27-30.

[5] Zhang B T, Pi Y G. Fractional order fuzzy sliding mode control for permanent magnet synchronous motor servo drive. Control and Decision, 2012, 27(12): 1776-1780.

[6] Wang L Q, Lu Q F, Ye Y Y, et al. Fuzzy-PI regulated field oriented control of linear induction motor in urban transit. Control Theory & Applications, 2009, 26(7): 734-738.

[7] Mei C L, Huang W T, Yin K T, et al. Speed egulating system for induction motor and inverter Based on Hammerstein model Neural network control. Control and Decision, 2015, 30(6): 1148-1152.

[8] Utkin V I. Sliding mode control design principles and applications to electric drives. IEEE Transactions on Industrial Electronics, 1993, 40(1): 23-36.

[9] Chern T L, Wu Y C. Design of integral variable structure controller and application to electrohydraulic velocity servo systems. IEE Proceedings D, 1991, 138(5): 439-444.

[10] Tan J, Zhou Z, Zhu X P, et al. Attitude control for flying wing unmanned aerial vehicles based on fractional order integral sliding-mode. Control Theory & Applications, 2015, 32(5): 607-614.

[11] Miao Z C, Dang J W, Ju M, et al. Induction motor sensor-less vector control based on fractional order integral sliding mode observer. Electric Machines and Control, 2018, 22(5): 84-93.

[12] Zhang B T, Gao F R, Yao K. Neural network and adaptive algorithm-based fractional order slidingmode controller. Control Theory & Applications, 2016, 33(10): 1373-1377.

[13] Miao Z C, Zhang W B, Han T L. Fractional order integral sliding mode control for PMSM based on fractional order sliding mode observer. Journal of Measurement Science and Instrumentation, 2019, 10(4): 389-397.

[14] Monje C A, Chen Y Q, Vinagre B M, et al. Fractional-order systems and controls: fundamentals and applications. Springer Science & Business Media, 2010.

[15] Ruan Y, Chen B S. Control system of electric drives motion control system. Beijing: China Machine Press, 2009.

[16] Li Z, Hu G D, Cui J R, et al. Sliding-mode variable structure control with integral action for permanent magnet synchronous motor. Journal of China Electromechanical Engineering, 2014, 34(3): 431-437.

矿用机车牵引电机非线性动态分数阶滑模控制

张海明[1]，缪仲翠[2]，张　鑫[2]

（1. 兰州交通大学 机电工程学院，甘肃 兰州 730070；
2. 兰州交通大学 自动化与电气工程学院，甘肃 兰州 730070）

摘　要： 矿用电机车恶劣的运行环境和复杂的运行工况会影响机车牵引电机控制性能。为了提高电机车牵引电机的速度控制性能，提出了一种考虑不确定因素的动态分数阶积分滑模控制算法。针对牵引电机复杂的负载扰动设计了负载转矩滑模观测器，将其观测值融入到动态分数阶滑模控制器中，以克服负载扰动对控制性能的影响。然后，应用 Lyapunov 定理证明了所设计控制器的稳定性，并将所设计的动态分数阶滑模控制器与整数阶滑模、分数阶滑模控制进行了仿真实验对比。仿真实验表明，相比于整数阶滑模和分数阶滑模控制器，带负载观测的动态分数阶积分滑模控制器的动态性能和静态性能更好，并有较强的抗干扰能力，可以有效地提高矿用机车牵引电机的控制性能。

关键词： 矿用牵引电机；分数阶滑模；负载观测器；动态分数阶滑模控制

引用格式： ZHANG Hai-ming, MIAO Zhong-cui, ZHANG Xin. Nonlinear dynamic fractional sliding mode control to the motor of mining locomotive. Journal of Measurement Science and Instrumentation, 2020, 11(4): 373-381. [doi: 10.3969/j.issn.1674-8042.2020.04.009]